Available online at www.sciencedirect.com
ScienceDirect
European Journal of Mechanics B/Fluids 27 (2008) 579–590

Linear stability of channel entrance flow

Damien Biau

DICAT, University of Genova, Via Montallegro 1, 16145 Genova, Italy

Received 12 October 2006; received in revised form 1 October 2007; accepted 11 November 2007

Available online 26 December 2007

Abstract

The spatial stability of two dimensional, steady channel flow is investigated in the downstream entry zone for both exponentially and algebraically growing disturbances. A model based on previous work is presented for the base flow which represents a small deformation of plane Poiseuille flow. The base flow evolution towards the fully developed state comes from the experimental and theoretical study of M. Asai and J.M. Floryan [M. Asai, J.M. Floryan, Certain aspects of channel entrance flow, Phys. Fluids 16 (2004) 1160–1163]. This flow is found to be more stable than the parabolic Poiseuille flow. The most destabilizing base flow defect is then calculated using a variational method. The compromise between the destabilizing effect of the defect, which diffuses downstream, and the instability growth is found to be insufficient to provoke transition in the downstream laminar flow.

PACS: 47.15.Fe; 47.20.-k; 47.27.nd

Keywords: Hydrodynamic instability; Channel flow

1. Introduction

This work is concerned with the stability properties of entry channel flow. The disturbance growth mechanism in parallel and quasi-parallel flows is of great interest to understand transition to turbulence and has been the object of several theoretical and experimental studies.

For simple shear flow cases, such as the Poiseuille flow, the experimental flow behavior and the theoretical results are quite different. Transition to turbulence is observed for minimum Reynolds number (based on the half channel height and the centreline velocity) around $Re = 1000$ (Nishioka and Asai [12]), well below the critical value provided by linear stability theory, i.e. $Re_c = 5772$ (Orszag [13]). The transition may occur at Reynolds number lower than 5772 because of the subcritical character of the instability.[1]

The stability characteristics of shear flows are extremely sensitive to external perturbations. This property, linked to the non-normal nature of the dynamical disturbances operator, is crucial in determining the outcome of laboratory experiments. Research on the topic of transition in shear flows in the last ten years has been concerned particularly

E-mail address: biau@diam.unige.it.

[1] The subcritical transition cannot be attributed to the finite spanwise size of the channel. Tatsumi and Yoshimura [17] have investigated the linear stability of Poiseuille flow in a rectangular duct. The critical Reynolds number increases monotonically while decreasing aspect ratio. For large channel, the asymptotic value is in agreement with the infinite one (i.e. $Re_c \to 5772$).

0997-7546/$ – see front matter
doi:10.1016/j.euromechflu.2007.11.004

with identifying worst case scenarios, i.e., those initial (or inlet) conditions responsible for the largest growth of disturbances, in a linearized setting. The disturbance can be distinguished by their growth: exponential or algebraic. The physical mechanisms describing the origin of disturbance growth may be extracted from the Reynolds–Orr equation describing the time evolution of the fluctuations kinetic energy E. For a parallel shear flow $U(y)$ this equation is written:

$$\frac{dE}{dt} = -\int_y U_y \langle uv \rangle \, dy - \frac{1}{Re} \int_y \left\langle (\nabla \times \vec{\mathbf{u}}) \right\rangle dy, \tag{1}$$

where $\langle \cdot, \cdot \rangle$ designs an averaged value in streamwise and spanwise directions. A perturbation can be amplified if the production term $-\int_y U_y \langle uv \rangle \, dy$ overcome the dissipation $-\frac{1}{Re} \int_y \langle (\nabla \times \vec{\mathbf{u}}) \rangle \, dy$. This equation permits a general point of view on the different mechanism of instability. The production term can be positive in two manners. First the phase shift at the wall between the streamwise and wall normal velocity perturbations implies a constructive interaction at the origin of exponentially growing Tollmien–Schlichting waves. Alternatively, by the lift-up mechanism, wall normal fluctuation induces streamwise velocity fluctuation or streaks (Butler and Farrell [4], Trefethen et al. [18]). This lift-up mechanism implies algebraic amplification, which scales with the Reynolds number.

If a perturbation attains – even if only transiently – a sufficiently large amplitude, some non-linear boot-strapping effect will bring the system to transition. This interpretation of linear stability theory has led many scientists studying transition in shear flows to almost abandon the traditional single-mode growth of the linear stability approach which captures the asymptotic behavior of the system, to pursue studies of non-modal transient growth, optimal perturbations, and pseudospectra. The concept of tree-dimensional optimal disturbances has been introduced by Butler and Farrell [4] and pursued by many others. All of the studies on optimals in wall-bounded shear flows (whether temporal or spatial) have shown that streamwise vortices transform into streaks downstream (in time or space) and that the disturbance energy, mostly carried by the streaks, can grow by orders of magnitudes over its initial value. The recent book by Schmid and Henningson [16] provides a complete account of the recent view of transition.

In this article we are interested on the influence of weak base flow distortions on linear stability results. The base flow uncertainty of the stability equation can be represented with δU, a possibly finite, but typically small, distortion of the idealized base flow U_{ref} (i.e.: $U = U_{\text{ref}} + \delta U$). The δU-pseudospectrum, introduced by Bottaro et al. [3], is defined as

$$\Lambda_{\delta U}(L) = \left\{ \alpha \in \mathbb{C} \colon \epsilon \in \Lambda\big(L(U_{\text{ref}} + \delta U)\big), \text{ for some } \delta U \text{ with } \|\delta U\| \leqslant \epsilon \right\},$$

where $\Lambda(L)$ is the spectrum of the linear stability operator L. The spectrum of $L(U + \delta U)$, is a subset of the unstructured pseudospectrum studied by Trefethen et al. [18]. It is well known that the pseudospectrum of a hydrodynamic stability operator can significantly deviate from its spectrum when the operator is non-normal, indicating the strong sensitivity of non-normal operators to external excitations, and the consequences of this fact in hydrodynamic stability theory have been explored in details in a seminal paper by Trefethen et al. [18]. In particular, it has been shown that the pseudospectrum can protrude far into the unstable half plane for nominally subcritical conditions. The most destabilizing distortion, the so-called *minimal defect*, can be calculated by a variational approach. This problem has been recently addressed in the temporal setting by Bottaro et al. [3] for Couette flow and in the spatial setting by Gavarini et al. [6] for pipe Poiseuille flow. The approach has been extended by Hwang and Choi [8] to the case of a two-dimensional wake in order to suppress or enhance the absolute instability.

The main objective of the present work is to investigate the stability properties of two-dimensional, steady entry flow, for both exponentially and algebraically growing disturbances. The paper is organized as follows. The model of entry flow is described in Section 2. The following section is dedicated to the linear stability analysis of realistic entry flow accruing from experiments by Asai and Floryan [1]. In the last section the worst possible entry flow is identified, for subcritical values of the Reynolds number, by optimization method.

2. Base flow defect formulation

The channel flow induced by a streamwise pressure gradient is considered. The mean velocity is made dimensionless using the maximum velocity U_0, the vertical distance scales with the half-channel height h, so that the fully developed base flow reads $U_{\text{ref}}(y) = 1 - y^2$. In this section we present a model of the channel entry flow, downstream

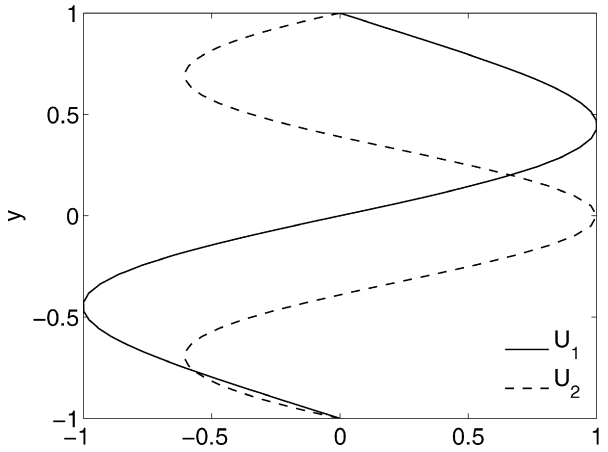

Fig. 1. Streamwise velocity deviation corresponding to the first and second eigenfunctions of Eq. (3), normalized with their maximum.

of the channel inlet, where the evolution has a universal character. Recent review of the relevant literature as well as a detailed description of the flow, in the case of channel entrance with sharp corners, are given in reference [15].

We take as a characteristic streamwise scale $L = h\,Re$, as in Prandtl's boundary layer approximation. This is the only difference with the model presented by Sadri and Floryan [15] and Asai and Floryan [1]. By proceeding as we do, the Reynolds number is scaled out in the dimensionless equations. From the physical point of view, the normal direction is characterized by diffusive effects and the longitudinal direction is dominated by advection, which justifies the Reynolds number in the ratio of the different characteristic lengths. By scaling the normal coordinates y with h, the streamwise coordinate x with $h\,Re$, and the streamwise velocity with U_0, it follows that U_0/Re should be used as the scale for the normal velocity V. The pressure is normalized by $\rho(U_0/Re)^2$, with ρ the density of the fluid.

The dimensionless mean flow (U, V, P), supposed to be two-dimensional and stationary, may be represented as a steady deviation superposed to the fully developed Poiseuille flow $U_{\mathrm{ref}} = 1 - y^2$, $V_{\mathrm{ref}} = 0$, $dP_{\mathrm{ref}}/dx = 2/Re$):

$$\begin{aligned} U(x, y) &= U_{\mathrm{ref}}(y) + \sum \kappa_n U_n(y) e^{\lambda_n (x - x_0)}, \\ V(x, y) &= \sum \kappa_n V_n(y) e^{\lambda_n (x - x_0)}, \\ dP/dx &= dP_{\mathrm{ref}}/dx + \sum \kappa_n P_n e^{\lambda_n (x - x_0)}. \end{aligned} \tag{2}$$

The streamwise coordinate could be translated along x so that we can introduce a fictitious origin x_0. In the following x_0 is fixed to zero. The flow is supposed to be slightly perturbed from plane Poiseuille flow, so the equation describing the dynamics of the disturbance is be linearized around the mean state $(U_{\mathrm{ref}}, P_{\mathrm{ref}})$. This equation for the streamfunction, defined by $\psi_n' = U_n$, $-\lambda_n \psi_n = V_n$, takes the form of a generalized eigenvalues problem:

$$\frac{d^4\psi_n}{dy^4} - \lambda_n \left(U_{\mathrm{ref}} \frac{d^2\psi_n}{dy^2} - U_{\mathrm{ref}}'' \psi_n \right) = 0, \tag{3}$$

associated with homogeneous Dirichlet and Neumann boundary conditions: $\psi_n = \psi_n' = 0$ for $y = \pm 1$. The first two modes are $\lambda_1 = -21.680/Re$, $\lambda_2 = -28.221/Re$ and correspond, respectively, to sinuous (antisymmetric) and varicose (symmetric) modes, cf. Fig. 1.

The particular case $dP/dx = 0$, corresponding to a sinuous disturbance, leads to a Sturm–Liouville problem. In this form the projection weights κ_n are simply determined by an appropriated scalar product; details are given in Appendix A.

3. Linear stability of Asai and Floryan [1] experimental flow

The model for the base flow measured by Asai and Floryan [1] is used. The contraction section used in the experiment is symmetric with respect to the midplane of the channel. So measurements show a deviation shape very similar to mode 2 in expansion (2) (i.e. $\kappa_2 \gg \kappa_n$, for $n = 1, 3, 4, 5, \ldots$).

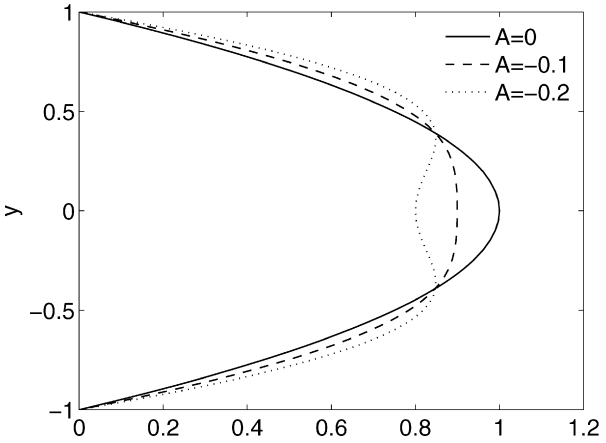

Fig. 2. Base flow profiles for different disturbance amplitudes.

$$U(x,y) = U_{\text{ref}}(y) + AU_2(y)e^{\lambda_2 x},$$
$$V(x,y) = AV_2(y)e^{\lambda_2 x},$$
$$dP/dx = dP_{\text{ref}}/dx + A_P e^{\lambda_2 x}. \tag{4}$$

A quantifies the deviation from Poiseuille flow. Some base flow profiles are presented in Fig. 2. Asai and Floryan [1] give a relation between the velocity amplitude A and the pressure amplitude as $A_P = -A/Re\, d^2U_2/dy^2|_{y=-1}$.

3.1. Modal analysis

First, we study the evolution of disturbances with a modal analysis based on the parallel flow assumption. This classical stability analysis is focused on the sign of the least stable mode, labeled as Tollmien–Schlichting mode, which is expressed in wave like form in homogeneous directions as: $q(y)e^{i(\alpha x+\beta z-\omega t)}$. The interpretation of the results depends on how the governing equations are solved. Three type of analysis can be used. The analysis making the complex frequency ω the eigenvalue, fixing the streamwise wave number is called a temporal stability analysis. On the other hand, if ω is fixed real and α is the eigenvalue, a spatial stability analysis is performed. If the relationship between α and ω is restricted such that the combination of both value defines a point of vanishing group velocity, the resulting analysis determines the absolute stability of the flow field.

In temporal stability analysis, the disturbance is applied in space and observed as it evolves in time. The stability of the flow is indicated by the imaginary part defining the growth rate of the disturbance whereas the real part defines the circular frequency. Temporal stability analysis was the first type of linear stability analysis performed in flows, in part because computationally these calculations are easier to carry out. In spatial stability analysis, the disturbance is applied in time and the evolution of the disturbance is observed in space. Spatial stability result can thus be easily compared to experimental results where usually the flow is excited at a point and the effects of the excitation is studied as the flow evolves downstream. In addition to these two types, absolute stability analysis is an important tool. An absolutely unstable flow field will not allow excitation of any other modes and instead behave like a self-excited oscillator. To determine absolute stability, all points with vanish group velocity are found. If any of these points are found to have a positive temporal growth rate, the flow is absolutely unstable. The saddle point condition is expressed mathematically by: $\frac{d\omega}{d\alpha}(\alpha_0) = 0$. An upstream mode is a mode whose group velocity is negative with respect to the base flow direction. A downstream mode corresponds to positive group velocity.

The approach adopted here is spatial, implying that the eigenvalue problem is solved for $\alpha \in \mathbb{C}$ with ω and β real. In compact form this system can be noted as $\mathcal{L}\tilde{q}_n = \alpha_n \tilde{q}_n$. The modal stability, for arbitrary base flow distortion, was studied earlier by Hidfi et al. [7]. The work of these authors has been conducted in the temporal framework, which is simpler but not as physically relevant as the spatial framework for the kind of open flows examined here. Although the neutral curve is independent of a spatial or temporal viewpoint, these two problems are quite different, because the spatial problem is elliptic. In fact, with the possible exception of the unstable mode, the upper half of the complex α-plane contains downstream decaying modes while the lower half corresponds to upstream decaying modes. The

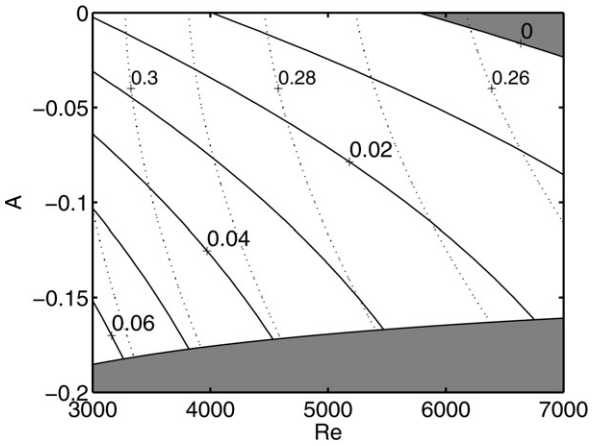

Fig. 3. Growth rate *imag*(α) of TS mode (continuous lines) and corresponding phase velocity c (dotted lines) in Reynolds number Re versus the amplitude A plane. The shaded regions are unstable.

spatial approach permits a direct comparison between the streamwise evolution of the base flow and the growth of the unstable mode.

Using Squire theorem, the modal analysis can be reduced to the Orr–Sommerfeld equation with $\beta = 0$:

$$\left\{\left(-i\omega + i\alpha U - \frac{1}{Re}\nabla^2\right)\nabla^2 - i\alpha U''\right\}v = 0. \tag{5}$$

The growth rate and corresponding phase velocity $c = \omega/\alpha_r$ contours, in the (Re, A) plane, are displayed in Fig. 3.

The distortion on the entry flow displays a stabilizing effect on the viscous instability (Tollmien–Schlichting waves). For undisturbed Poiseuille flow, the critical Reynolds number is 5772. This threshold increases with the defect's amplitude. In addition, for high distortions an inviscid instability appears, linked to an inflection point of the mean velocity profile. This inviscid unstable mode is solution of Rayleigh's equation:

$$\left\{(-i\omega + i\alpha U)\nabla^2 - i\alpha U''\right\}v = 0. \tag{6}$$

The flow present an unstable inviscid mode for amplitude A lower than -0.11. The associated phase velocity is larger than for the viscous Tollmien–Schlichting modes $c(\omega) = \omega/\alpha_r \approx constant = 0.85$.

3.2. Transient growth

As a next step, we investigate an algebraically growing perturbations, that cannot be attributed to single-mode exponential growth. The search for initial condition for transiently growing perturbations usually starts with the search of optimal perturbation, i.e. the search of the inlet condition that provides the largest energy growth. Consequently, we define the maximum kinetic energy amplification $G_{\max}$ as,

$$G_{\max} = \max_{\forall x \in [0;\infty[} \left\| q(x) \right\|_E,$$

with the normalization, $\|q(0)\|_E = 1$. The subscript E denotes an energetic norm defined, in continuous and discrete form, as:

$$\frac{G}{Re^2} = \frac{\int_{-1}^{+1} u^2\, dy|_{x=x_{\text{opt}}}}{\int_{-1}^{+1} v^2 + w^2\, dy|_{x=x_0}} = \frac{q^T H_{\text{out}} q|_{x=x_{\text{opt}}}}{q^T H_{\text{in}} q|_{x=x_0}}. \tag{7}$$

The disturbances corresponding to this maximum take the form of streamwise elongated and steady structures. In this case the parallel base flow assumption is no longer valid and the characteristic scales for the perturbation must be identical to those for the base flow defined in Section 2. The algebraically growing perturbations can be adequately described by the use of linearized equations in which the long scale ($h\,Re$) is used to normalize streamwise length, and the short scale (h) is used for the cross-stream directions. Applying these scales to the linearized Navier–Stokes

equations it follows that the disturbance equations, at leading order, are independent of the Reynolds number and parabolic in the streamwise direction. Moreover, the linearization permits a mode-by-mode study in Fourier space. Along the homogeneous directions the perturbations are expressed in Fourier-like form: $\exp(i\beta z - i\omega t)$. Finally, the disturbance equations take the symbolic form $Aq_x = Bq$, which in expanded form, read:

$$\begin{aligned}
&u_x + v_y + i\beta w = 0,\\
&-i\omega u + (Uu)_x + Vu_y + U_y v = u_{yy} - \beta^2 u_{zz},\\
&-i\omega v + (Vu + Uv)_x + 2(Vv)_y + i\beta V w = -p_y + v_{yy} - \beta^2 v_{zz},\\
&-i\omega w + (Uw)_x + (Vw)_y = -i\beta p + w_{yy} - \beta^2 w_{zz}.
\end{aligned} \tag{8}$$

These equations are associated to homogeneous Dirichlet boundary conditions at the walls. This system was previously used by Luchini [11] for optimal perturbations in non-parallel boundary layer. The inflow condition for Eqs. (8) was computed using the discrete Lagrange multipliers method: a Lagrangian functional is defined as

$$\mathcal{L} = \frac{G(L)}{Re^2} + \int_0^L \bar{p}^T \big[(Aq_x) - Bq\big]\, dx,$$

maximization of $\mathcal{L}$ leads to the unconstrained set of equations:

$$\begin{aligned}
&q(x=0,y) = AH_{\text{in}}^{-1} p(x=0,y),\\
&(Aq)_x = Bq,\\
&p(x=L,y) = (\bar{A}^T)^{-1} H_{\text{out}} q(x=L,y),\\
&\bar{A}^T p_x = -\bar{B}^T p.
\end{aligned} \tag{9}$$

The perturbations are normalized such that the inflow energy is equal to one. The equations are discretized using a Chebyshev collocation method in the wall normal direction and a finite difference scheme in the streamwise direction. The iterations are pursued until the subsequent changes in the maximal gain dropped below a threshold value, fixed at 10^{-4}. The parameters ω_{opt}, β_{opt} and x_{opt}, corresponding to the largest possible gain, at fixed Reynolds number and amplitude, are obtained using a shooting method. The optimal frequency was found to vanish in all cases. The maximum gain $G_{\max}/Re^2$ and corresponding β_{opt} and x_{opt} are drawn in Fig. 4 as function of the initial defect amplitude.

The streaks presents a weak sensitivity to the mean flow distortion, in contrast to TS waves. When the defect amplitude increases, the streaks maximum amplitude decreases slowly. Simultaneously, the corresponding location decreases and the streaks' width increases. An example of optimal perturbation is presented in Fig. 5.

The optimal perturbations in the entry channel flow are very similar to those found for the unperturbed Poiseuille flow (cf. Biau and Bottaro [2]).

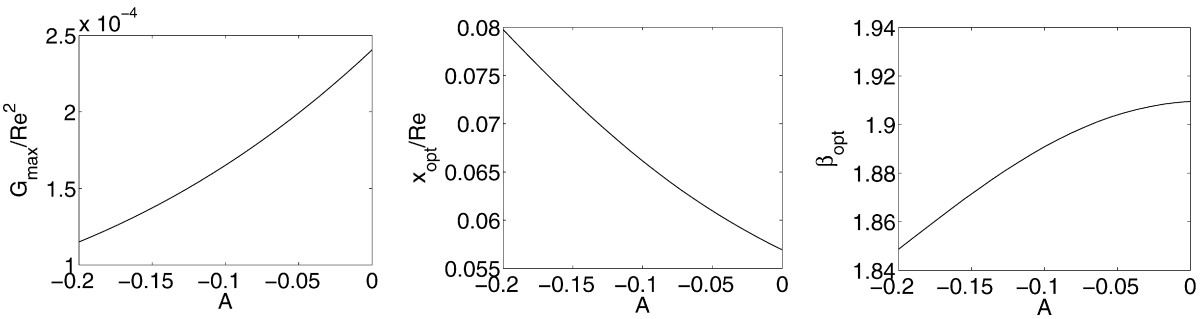

Fig. 4. Maximum gain (G), optimal streamwise location x_{opt} and optimal spanwise wave number (β) versus the amplitude A.

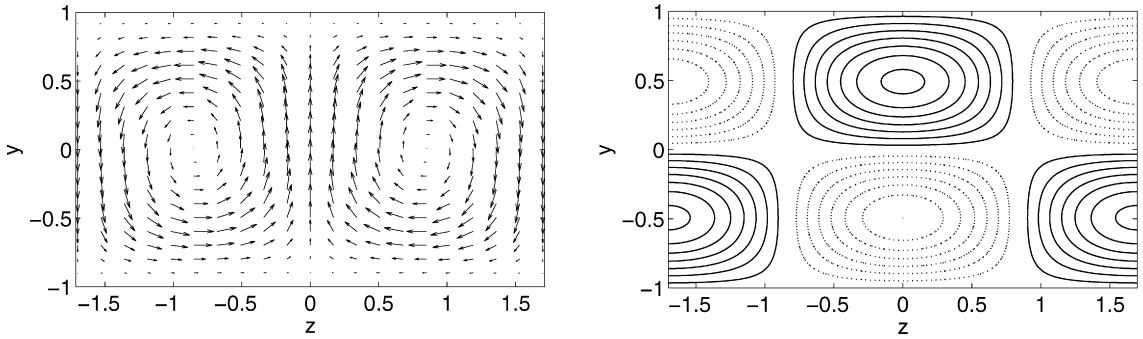

Fig. 5. Optimal inflow disturbances at $x = 0$ (left) and resulting streaks at $x = x_{\text{opt}}/Re$ (right) for $A = -0.2$. The inflow perturbation is represented through the cross-stream velocity (vectors). The outflow is displayed with isolines of the streamwise velocity; the positive and negative values are respectively denoted by continuous and dotted lines.

4. Worst-case scenario

In the previous sections the stability properties of realistic entry flows was investigated. The results show a net stabilizing effect. Now we are interested in finding the worst, most destabilizing, flow distortion, following the method developed by Bottaro et al. [3]. Bottaro et al. described a technique, in the temporal framework, to identify optimally configured defects of the base flow capable of rendering Couette flow linearly unstable. The work has been extended to the spatial frame by Gavarini et al. [6] for the case of pipe Poiseuille flow. This work has shown that the optimal base flow distortion is efficient to provoke transition in laminar pipe flow. Hwang and Choi [8] have investigated the effect of basic-flow modification on the absolute instability in a wake at low Reynolds number. Using the method of calculus of variation, they optimally modify the basic flow to suppress or enhance the absolute instability. For a two-dimensional parallel model wake and a circular-cylinder wake, this work shows that the positive and negative velocity perturbations to the basic flows, respectively, at the wake centreline and separating shear layer suppress the absolute instability. Here, the same technique is used for entry channel flow in subcritical conditions, by considering disturbances developing in space.

The deviation from the undisturbed Poiseuille flow is quantified by a kinetic energy norm:

$$\epsilon = \int_y \big(U(x=0,\, y) - U_{\text{ref}}(y)\big)^2\, dy. \tag{10}$$

The laminar basic flow is specified by projection on the set of eigenfunction defined in Section 2, Eq. (2). The inflow distortion $\delta U(x = 0, y)$ is obtained by an optimization method. The mean velocity profiles are available at any streamwise location (x) using the discrete projection:

$$\delta U(x, y) = \sum_n \mathbb{Q}_n(\kappa_n e^{-\lambda_n x}) \quad \text{with } \kappa = \mathbb{Q}^{-1}\delta U(x = 0, y). \tag{11}$$

The matrix $\mathbb{Q}$ is constituted by the eigenfunctions of Eq. (3), i.e. $\mathbb{Q}_{nm} = U_n(y_m)$.

4.1. Modal analysis

Operators resulting from perturbations of the base flow are subject to Squires theorem and transformation. Hence, we limit ourselves here to considering only the Orr–Sommerfeld equation. An infinitesimal, locally parallel variation δU in the Poiseuille flow, injected into the Orr–Sommerfeld equation, symbolically written as $\mathcal{L}_{OS}$, leads to:

$$\mathcal{L}_{OS}(U + \delta U; \alpha + \delta\alpha)(\mathbf{v} + \delta\mathbf{v}) = 0, \tag{12}$$

which can be rewritten, after linearization, as:

$$\mathcal{L}_{OS}\delta\mathbf{v} + \delta U \frac{\partial \mathcal{L}_{OS}}{\partial U}\mathbf{v} + \delta\alpha \frac{\partial \mathcal{L}_{OS}}{\partial \alpha}\mathbf{v} = 0. \tag{13}$$

In order to isolate the eigenvalue variation, we now project onto the adjoint subspace spanned by $a(y)$, with the scalar product $(\cdot,\cdot)$ defined by $(p,q)=\int_y p^* q\,dy$. The function $a(y)$ is solution of the adjoint Orr–Sommerfeld equation:

$$\mathcal{L}_{OS}{}^{\dagger}\mathbf{a}=\left\{\left[-i\omega+i\alpha^* U+\frac{1}{Re}\nabla^2\right]\nabla^2+2i\alpha^* U'\partial_y\right\}\mathbf{a}=0, \tag{14}$$

with homogeneous Dirichlet and Neumann boundary conditions. The variation in a given eigenvalue arising from an arbitrary variation δU is:

$$\delta\alpha=\int_{-1}^{+1} G_U\delta U\,dy, \tag{15}$$

where the sensitivity function G_U is an appropriate combination, after integration by parts, of direct and adjoint eigenfunctions of the given mode:

$$G_U=\alpha\mathbf{a}^*\nabla^2\mathbf{v}-\alpha(\mathbf{a}^*\mathbf{v})'', \tag{16}$$

with the direct-adjoint normalization:

$$-(\mathbf{a},\partial_\alpha L_{OS}\mathbf{v})=\int_{-1}^{1}\mathbf{a}^*\left[U''+2\alpha(\alpha U-\omega)+\left(\frac{4i\alpha}{Re}-U\right)\nabla^2\right]\mathbf{v}\,dy=1.$$

Using Lagrange multipliers and following the method described in Bottaro et al. [3], we obtain:

$$\begin{cases} U=U_{\text{ref}}+\frac{\text{Im}(G_U(x=0,y))}{2\lambda}, \\ \lambda=-\sqrt{\frac{1}{4\epsilon}\int_y(\text{Im}(G_U(x=0,y)))^2\,dy}. \end{cases}$$

For the case of undisturbed Poiseuille flow, the shape of the sensitivity function ($\text{Im}(G_U)$) shows that Tollmien–Schlichting mode is mostly sensitive to near-wall symmetric forcing of the mean flow. The most sensitive mode, which maximizes the imaginary part of the sensitivity function $\|\text{Im}(Gu)\|_\infty$ with respect to ω, is followed during the iterative process. The final results do not appear to depend on the choice of the tracked mode (for example some computations have been done with the least stable mode leading to the same final pseudo-mode). The results are presented in Fig. 6, where the growth rate is represented in the plane Reynolds number, in the range $1000<Re<4000$, versus amplitude of the defect, in the range $5\times10^{-6}<\epsilon<10^{-4}$. The minimum energy threshold satisfies the Re^{γ}-scalings, with $\gamma=-3/2$; corresponding to $\gamma=-3/4$ for the amplitude threshold.

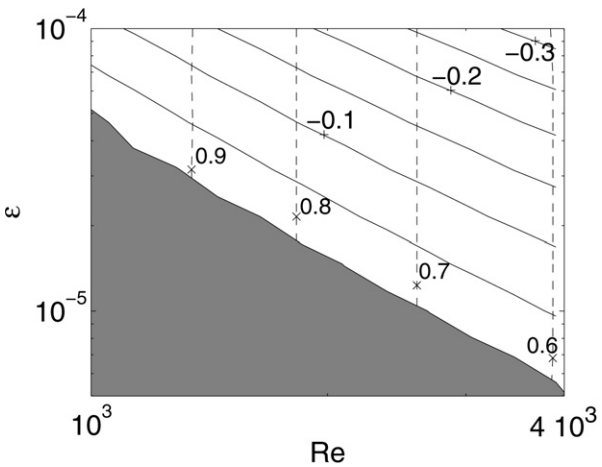

Fig. 6. Iso-α_i (continuous lines) in Reynolds number (Re) and defect energy norm (ϵ) plane. The stable domain is shaded. The dashed lines are isolines of the frequency ω of the most unstable mode.

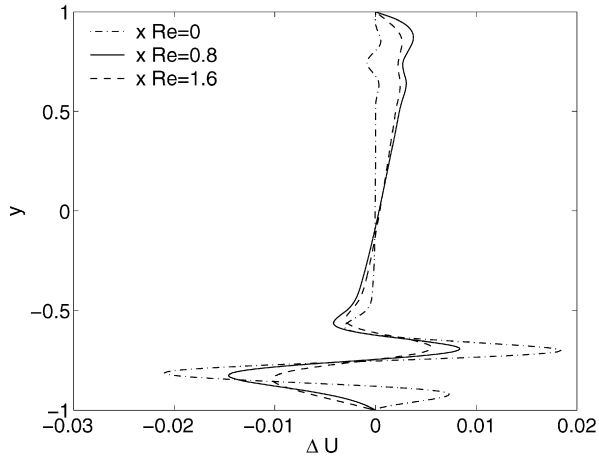

Fig. 7. Minimal defect for $Re = 2000$, $\epsilon = 5 \times 10^{-5}$ and $\omega = 0.773$ at various dowstream locations.

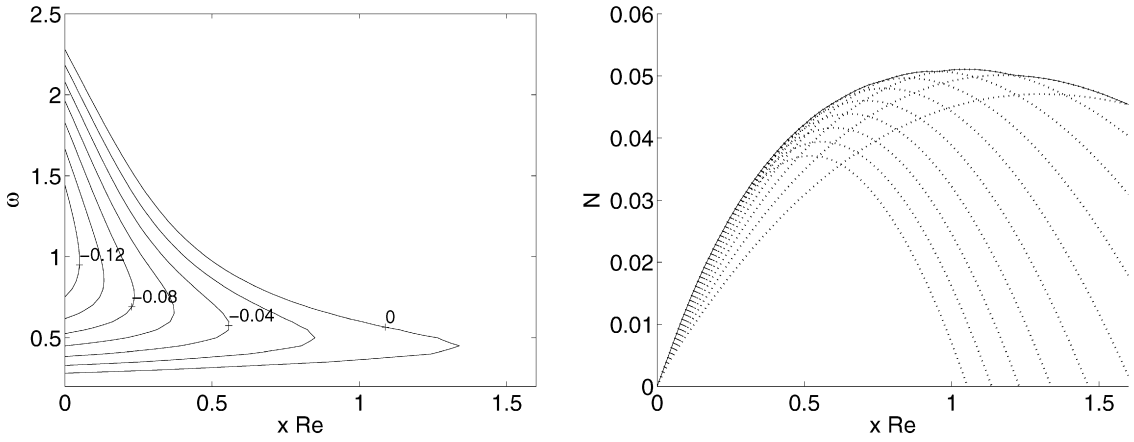

Fig. 8. Iso-growth rate (α_i) for $Re = 2000$, $\epsilon = 5 \times 10^{-5}$. Associated N factor for $\omega = 0.5, 0.55, \ldots, 1$.

In dynamical system point of view, the basin of attraction of laminar state shrinks for large Re as Re^{γ} say with $\gamma < 0$, so that small but finite perturbations lead to transition. Some authors have tried to describe this property with a scaling law with the amplitude of the perturbation triggering transition obeying a power law (Re^{γ}) with negative γ value. Trefethen et al. [18], by using arguments based on dominant balance of non-normal growth and non-linear-feedback conjectured that $\gamma < -1$. Chapman [5], through a formal asymptotic analysis of the Navier–Stokes equations, found that for streamwise initial perturbations $\gamma = -3/2$ (factoring out the unstable modes), while for oblique initial perturbations $\gamma = -5/4$. An experimental evidence for the value of $\gamma = -3/2$ for channel flow is proposed by Philip et al. [14]. The disturbance amplitude (the $\mathcal{H}_\infty$ norm) varies like $Re^{-3/2}$ in agreement with the theoretical value obtained by Chapman. The discrepancy between the value found here and the previous one probably comes from the two-dimensional assumption for the mean flow defect.

Some representative deviation shapes are plotted in Fig. 7.

The mean flow defect is damped downstream so the resulting instability results from the balance between the base flow defect diffusion against the growth of the instability. In order to compare these two phenomenon the so-called e^N method is used. The case is considered of $Re = 2000$ and $\epsilon = 5 \times 10^{-5}$; the corresponding optimal frequency is $\omega = 0.773$. A local stability analysis of this nearly parallel base flow is performed to determine the growth rate of the locally unstable disturbances for various frequencies ω and various streamwise locations. The stability diagram of amplified Tollmien–Schlichting waves as a function of the streamwise distance is depicted in Fig. 8 (left).

Let us consider now a wave which propagates downstream at a fixed frequency ω. The growth rate presented in Fig. 8 (left) shows that this wave is amplified up to a certain distance and is damped further downstream because of the

defect diffusing away. At any station $x > 0$, the wave amplitude A^{TS} can be related to its initial amplitude A_0^{TS} by the relation $A^{\mathrm{TS}}/A_0^{\mathrm{TS}} = \exp(\int_0^x -\alpha_i\, dx)$. The initial amplitude is linked to external noise through some receptivity mechanism. The streamwise variation of the natural logarithm $\ln(A^{\mathrm{TS}}/A_0^{\mathrm{TS}})$ is plotted in Fig. 8 (right) for several frequencies. The continuous line, representing the envelope of these curves, is called the N factor: $N = \max \ln(A^{\mathrm{TS}}/A_0^{\mathrm{TS}})$; $\forall\omega$. At each location, N represents the maximum amplification factor of the disturbances. As can be seen in Fig. 8 this amplification factor is too weak to overcome the viscous damping of the mean flow defect (Fig. 7), and the N-factor maintains very small values. For comparison purposes, in the Blasius boundary layer transition is triggered for $N = 9$.

4.2. Transient growth

To quantify the deviation from the undisturbed Poiseuille flow we use the previous definition of the kinetic energy (see Eq. (10)). The gain is defined with the energy transfer for the mean flow U to the disturbances: $-\int_{xy} uv\, dU/dy\, dy\, dx$; the Lagrangian functional is thus:

$$\mathcal{L} = -\int_{xy} uv\, \frac{dU}{dy}\, dy\, dx - \lambda\left(\int_y \left(U(x=0,y) - U_{\mathrm{ref}}\right)^2 dy - \epsilon\right).$$

Note that for computational convenience the gain is defined from a term which arises from the parallel flow assumption. We obtain:

$$\begin{cases} U = U_{\mathrm{ref}} + \frac{1}{2\lambda}\int_x \frac{\partial(uv)}{\partial y}\, dx, \\ \lambda = -\sqrt{\frac{1}{4\epsilon}\int_y \left(\int_x \frac{\partial(uv)}{\partial y}\, dx\right)^2}. \end{cases}$$

First the perturbations are optimized following Eqs. (9), then the base flow defect is optimized. The process is repeated until the subsequent change in the maximal gain dropped below a threshold value, fixed at 10^{-3}. The frequency ω

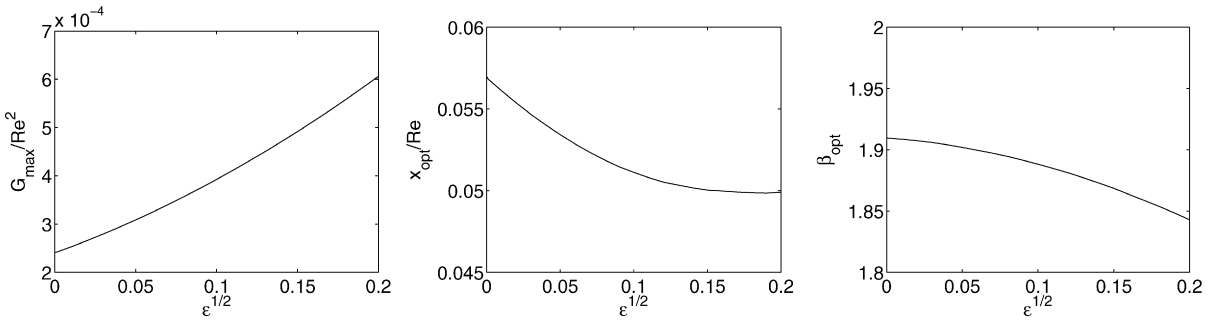

Fig. 9. Maximum gain (G), optimal streamwise location x_{opt} and optimal spanwise wave number (β) versus defect amplitude $\sqrt{\epsilon}$.

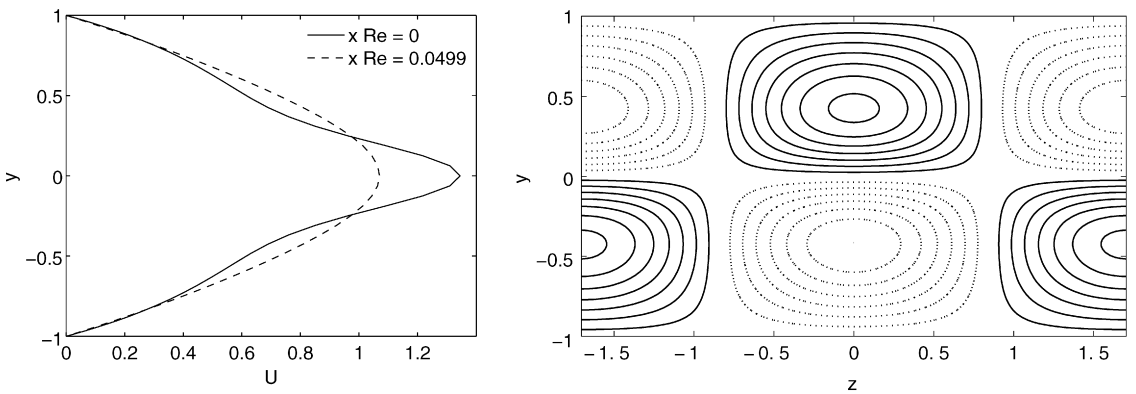

Fig. 10. Distorted base flow (left) and optimal streaks at $x = x_{\mathrm{opt}} = 0.0499$ (right); for $\epsilon = 0.04$, $\beta = \beta_{\mathrm{opt}} = 1.843$.

is fixed to zero in all cases. The maximum gain $G_{\max}/Re^2$ and corresponding β_{opt} and x_{opt} are drawn in Fig. 9 as function of the initial defect 'amplitude' $\sqrt{\epsilon}$.

The algebraically growing perturbations are weakly sensitive to base flow deviation, even for high defect amplitude. The gain is almost three times greater than in the Poiseuille case and the optimal streaks are slightly modified by the defect. The base flow distortion presents an increasing shear near the position of maximum amplitude of the streaks but is strongly damped downstream (Fig. 10).

5. Conclusions

In this study, spatial linear stability theory has been used to examine the stability of channel entrance flow. The presence of the entrance has a stabilizing effect in accordance with the well-know result that shear flows in a pressure drop region (accelerated flow) are more stable than those in the pressure decrease region (decelerated flow). For weak base flow distortion, in a negative pressure gradient (accelerated flow), the mean velocity profile has no inflection point and the instability – if it exists – is very weak. So the critical Reynolds number increases and the instability region decreases. For strong distortions, an inflection point gives rise to an inviscid instability described by Rayleigh theory. Secondly, the optimal distortion was determined, for both exponential and algebraic growing perturbations, but the instability growth is too weak to overcomes the viscous damping of the defect. Far downstream the defect is damped and critical values tend to the classical results for Poiseuille flow.

These conclusions are drawn under a strong hypothesis on the base flow distortion which is supposed to be weakly two-dimensional, i.e. depending on the wall normal coordinates with a slow streamwise variation. Work in progress focuses on two directions. First the stability of a base flow distortion which depends on spanwise coordinate, to try and capture the defect of minimal norm, taking the form of spanwise-periodic streaks, which could cause transition in subcritical duct flow. The final goal will be to compare and link such steady, finite amplitude structures to experimental observations of streaks and self-sustained structures in channel flows. Alternatively a streamwise influence coming from the leading edge induces a strong non-normality in the streamwise direction (global instability) which must influences the receptivity and instability process.

Acknowledgements

The author wishes to thank professor A. Bottaro for his helpful comments on this work. The financial support of the EU (program Marie Curie EST FLUBIO 20228-2006) is gratefully acknowledged.

Appendix A. Receptivity to inflow disturbances

For boundary layer flows, Libby and Fox [9] proposed a procedure to calculate the mode amplitude from an inflow condition imposed at x_0. Luchini [10] extended this results to overcome the leading edge singularity linked to algebraic form. In channel flow, without singularity at $x_0 = 0$, the Sturm–Liouville problem obtained for the auxiliary function $H = (\psi/U)'$ is:

$$(U^3 H')' + (3U''U^2 - \lambda U^4)H = 0, \tag{A.1}$$

with the associated orthogonality relation:

$$\int_{-1}^{1} H_k H_l \, dy = C_k \delta_{kl}, \quad C_k = \int_{-1}^{1} H_k^2 \, dy,$$

with δ_{kl} the Kronecker symbol. The defect is expanded in the form:

$$\delta\psi(x, y) = \sum_k A_k \psi_k(y) e^{\lambda(x - x_0)},$$

so that the amplitude A_k can be expressed using inflow condition:

$$A_k = C_k^{-1} \int_y \left(\frac{\delta U(x_0, y)}{U(y)} \right)' \left(\frac{\psi_k(y)}{U(y)} \right)' U^4 \, dy.$$

Moreover, multiplying Eq. (A.1) by ψ_k and integrating shows that eigenvalues λ are real and negatives, which implies that the base flow distortion is damped in the downstream direction.

References

[1] M. Asai, J.M. Floryan, Certain aspects of channel entrance flow, Phys. Fluids 16 (2004) 1160–1163.
[2] D. Biau, A. Bottaro, Optimal perturbations and minimal defects: Initial paths of transition to turbulence in plane shear flows, Phys. Fluids 16 (2004) 3515–3529.
[3] A. Bottaro, P. Corbett, P. Luchini, The effect of base flow variation on flow stability, J. Fluid Mech. 476 (2003) 293–302.
[4] K.M. Butler, B.F. Farrell, Three-dimensional optimal perturbations in viscous shear flow, Phys. Fluids 4 (1992) 1637–1650.
[5] S.J. Chapman, Subcritical transition in channel flows, J. Fluid Mech. 451 (2002) 35–97.
[6] M.I. Gavarini, A. Bottaro, F.T.M. Nieuwstadt, The initial stage of transition in pipe flow: Role of optimal base flow distortions, J. Fluid Mech. 517 (2004) 131–165.
[7] A. Hidfi, M.O. Touhami, J.K. Naciri, Channel entrance flow and its linear stability, J. Stat. Mech.: Theor. Exp. P06003 (June 1996).
[8] Y. Hwang, H. Choi, Control of absolute instability by basic-flow modification in a parallel wake at low Reynolds number, J. Fluid Mech. 560 (2006) 465–475.
[9] P.A. Libby, H. Fox, Some perturbation solutions in laminar boundary-layer theory, J. Fluid Mech. 17 (1964) 433–449.
[10] P. Luchini, Reynolds-number-independent instability of the boundary layer over a flat surface, J. Fluid Mech. 327 (1996) 101–115.
[11] P. Luchini, Reynolds-number-independent instability of the boundary layer over a flat surface: Optimal perturbations, J. Fluid Mech. 404 (2000) 289–309.
[12] M. Nishioka, M. Asai, Some observations of the subcritical transition in plane Poiseuille flow, J. Fluid Mech. 150 (1985) 441.
[13] S.A. Orszag, Accurate solution of the Orr–Sommerfeld stability equation, J. Fluid Mech. 50 (1971) 689.
[14] J. Philip, A. Svizher, J. Cohen, Scaling law for a subcritical transition in plane Poiseuille flow, Phys. Rev. Lett. 98 (15) (2007) 154502.
[15] R.M. Sadri, J.M. Floryan, Entry flow in a channel, Comp. Fluids 31 (2002) 133–157.
[16] P.J. Schmid, D.S. Henningson, Stability and Transition in Shear Flows, Springer-Verlag, New York, 2001.
[17] T. Tatsumi, T. Yoshimura, Stability of the laminar flow in rectangular duct, J. Fluid Mech. 212 (1990) 437–449.
[18] L.N. Trefethen, A.E. Trefethen, S.C. Reddy, T.A. Driscoll, Hydrodynamic stability without eigenvalues, Science 261 (1993) 578–584.